Wave farm impact on the beach profile: a case study 💬

J. Abanades[1*], D. Greaves[1], G. Iglesias[1]

[1] Plymouth University, School of Marine Science and Engineering, Marine Building, Drake Circus, Plymouth PL4 8AA, UK

ABSTRACT

If wave energy is to become a fully-fledged renewable, its environmental impacts must be fully understood. The objective of the present work is to examine the impact of a wave farm on the beach profile through a case study. The methodology is based on two coupled numerical models: a nearshore wave propagation model and a morphodynamic model, which are run in two scenarios, both with and without the wave farm. Wave data from a nearby coastal buoy are used to prescribe the boundary conditions. A positive effect on the wave climate, cross-shore sediment transport and, consequently, the evolution of the beach profile itself due to the presence of the wave farm was found. The wave farm leads to a reduction in the erosion of the beach face. This work constitutes the first stage of the investigation of the effectiveness of a wave farm as a coastal defence measure, and the accuracy of the quantification of the erosion reduction will be enhanced in future research. In any case, the overarching picture that emerges is that wave farms, in addition to providing carbon-free energy, can be used as elements of a coastal defence scheme.

Keywords: Wave energy; Wave farm; Wave Energy Converter; Nearshore impact; Beach profile; Erosion

---
*Corresponding author; e-mail: Javier.abanadestercero@plymouth.ac.uk, tel.: +44.(0)7583544041.

1. INTRODUCTION

Marine renewable energy and, in particular, wave energy is called to play a major role in achieving the renewable energy targets of the European Union for 2020 – the so-called 20-20-20 targets (European Commission, 2007). Among other advantages, wave energy boasts one of the highest energy densities of the renewable energy sector (Clément et al., 2002). At present, the main research areas in wave energy are: (i) the characterisation of the resource (Cornett, 2008; Iglesias and Carballo, 2009; 2010; 2011; Pontes et al., 1996; Vicinanza et al., 2013); (ii) the development of the technology (Falcão, 2007; Falcão and Justino, 1999; Kofoed et al., 2006); and, finally (iii) the environmental impact of wave farms, including the impact on the physical environment with which this work is concerned.

Knowledge of the impacts, positive or negative, is important for the development of the different types of marine energy because an Environmental Impact Assessment (EIA) is required for any such project. In the case of wave energy, the studies so far have dealt with the impact of a wave farm on the wave conditions in its lee. As waves propagate through the wave farm, their height is reduced according to an energy transmission coefficient. This coefficient depends on the performance of the Wave Energy Converters (WECs) selected. Millar et al. (2007) used SWAN (Booij et al., 1999), a phase-averaged spectral model, to quantify the impact on the wave climate and the shoreline changes for the Wave Hub project (UK). Notional values of the transmission coefficient (0, 40, 70 and 90%) were used due to the lack of information about the performance of the WECs at the time. In the same vein, Palha et al (2010) used the parabolic mid slope wave model REFDIF to perform a sensitivity analysis to study the impact on the shoreline using different layouts for the wave farm; and Vidal et

al. (2007) studied the impact of a small wave farm on the wave climate and the nearshore sediment transport.

Another line of work used physical modelling to investigate wave-WEC interaction. Carballo and Iglesias (2013) studied the modification of the nearshore wave climate using values of the energy transmission coefficient obtained from *ad hoc* physical model tests of a WaveCat WEC (Iglesias et al., 2008). Taking into account these values, a sensitivity analysis was performed with different layouts of the wave farm to assess its impact on the nearshore wave conditions. Mendoza et al. (2014) compared the impact of two wave farms with different WECs on the coastline. The results showed that a wave farm nearshore could produce accretion to some extent in some sections of the beach. In this context, Ruol et al. (2011), Nørgaard et al. (2011) and Zanuttigh and Angelelli (2013) put forward the idea of using a wave farm for shore protection based on the reduction of the nearshore wave height caused by the wave farm.

If a wave farm is to be used for the purpose of coastal protection, it is essential to understand its impact on the beach profile – an aspect of great practical relevance that has not been investigated so far. This is the main objective of the present work, which is conducted through a case study: Perranporth Beach.

Perranporth Beach is a 3 km sandy beach located in Cornwall, SW England (Figure 1). Composed of medium quartz sand (Austin et al., 2010), it has a semi-diurnal tidal regime and a tidal range of 6.3 m (macrotidal). The area has a great potential for wave energy (Thorpe, 2001) ; indeed, it was selected as the site for the Wave Hub Project, a grid-connected offshore facility for sea trials of WECs (Gonzalez et al., 2012; Reeve et al., 2011). The study covered the period from November 2007 to May 2008, corresponding to the part of the annual cycle with the highest frequency of storms based

on the onsite wave buoy data (Section 2.1). This time scale allows the assessment of the morphological changes in beaches, such as scarp formation, profile erosion and accretion, and bar evolution (Cowell and Thom, 1994).
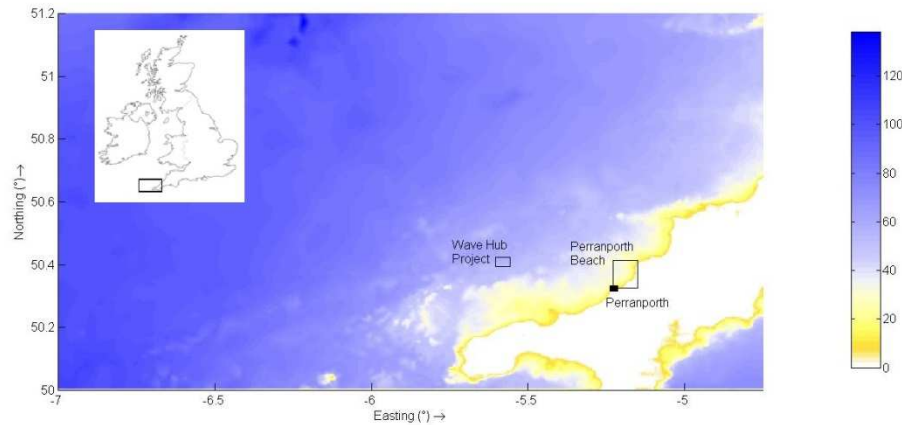

Figure 1 Bathymetry of SW England including the location of Perranporth Beach and the WaveHub Project [water depths in m].

Wave propagation was simulated using SWAN and the beach profile evolution with XBeach, a numerical model of nearshore processes (Roelvink et al., 2006). XBeach was successfully applied in a number of studies to describe the behaviour of beach profiles. Roelvink et al. (2009) assessed the beach erosion due to storms and McCall et al. (2010) focussed on the impact caused by hurricanes. Other authors, such as Jamal et al. (2011) and Williams et al. (2012) , used XBeach to investigate gravel beaches. More recently, Pender and Karunarathna (2012, 2013) demonstrated that XBeach is capable of modelling the medium-term evolution of the beach profile of a sandy beach. Their results showed a good fit to the measured profiles after each storm period. On these grounds, XBeach is used in the present work to compare the evolution of the beach profile with and without the presence of a wave farm situated close to Perranporth Beach.

This article is structured as follows. In section 2, the main characteristics of the data sets – which include wave, wind, tide and beach profile data – are presented, and the models are briefly described. This is followed by section 3, in which the results describing the impact of the wave farm on the wave conditions and the evolution of the beach profiles are presented and discussed. Finally, in Section 4, conclusions are drawn concerning the effects of a wave farm on the beach profile and, on these grounds, its applicability for coastal protection purposes.

2. MATERIALS AND METHODS

2.1 DATA

The wave data used for this study were hindcast and onsite wave buoy data. The directional wave buoy of the Coastal Channel Observatory located in front of Perranporth beach (Figure 2), in approximately 10 m of water depth with reference to the local chart datum (LCD), provided half-hourly data. The wave buoy data were used in conjunction with hindcast data from WaveWatch III, a third-generation offshore wave model consisting of global and regional nested grids with a resolution of 100 km (Tolman, 2002), to validate the high-resolution nearshore wave propagation model. In the period selected for the study, from November 2007 to April 2008, a number of storms with significant wave heights over 6 m occurred (Figure 5). The mean values of significant wave height, H_s, and peak wave period, T_p, were 2.4 m and 13 s, respectively. Given the orientation of the coastline and its exposure to the long Atlantic fetch, the relevant wave direction is from the IV quarter (from W to N), prevailing NW.

5
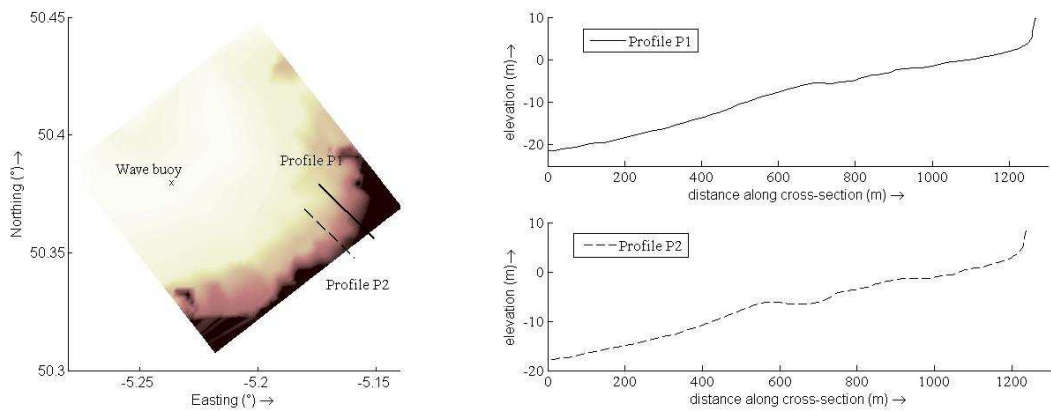
Figure 2 Initial beach profiles (P1 and P2) including their location and the position of the wave buoy. Water depth in relation to local chart datum

Wind data with a three-hourly frequency obtained from the Global Forecast System (GFS) weather model were used as input of the wave model. In the period covered in the study the mean wind velocity magnitude at a height of 10 m above the sea surface was $u_{10} = 9.5$ ms^{-1}. The strongest winds came from the NW, with u_{10} values exceeding 20 ms^{-1}.

The SW coast of England is characterised by a large tidal range, which may affect the beach morphodynamics. For this reason, the tide was included into the morphodynamic model with constituents obtained from the TPXO 7.2 global database, a global model of ocean tides that solves the Laplace equations using data from tide gauges and the TOPEX/Poseidon Satellite (Egbert et al., 1994) .

The beach profiles were obtained through field survey by the Coastal Channel Observatory. The initial profiles (Figure 2), typical of the end of summer at Perranporth Beach, are associated with less energetic wave conditions. The beach profile evolution is characterised during the summer by an increase of the sediment transport onshore. In contrast, offshore movement of sediment is the predominant phenomenon during the winter owing to the more energetic wave conditions, which results in a lowering of the

intertidal beach face. Indeed, most of the profile change at Perranporth Beach occurs in the lower intertidal to sub-tidal active regions (Scott et al., 2011).

2.2 *WAVE PROPAGATION MODEL*

The assessment of the wave height reduction on the shore due to the wave farm was carried out using SWAN (Simulating WAves Nearshore), a third-generation numerical wave model developed to model nearshore wave climate transformations. SWAN computes the evolution of the wave spectrum based on the spectral wave action balance equation,

$$\frac{\partial N}{\partial t} + \nabla \cdot \left(\vec{C} N \right) + \frac{\partial \left(C_\theta N \right)}{\partial \theta} + \frac{\partial \left(C_\sigma N \right)}{\partial \sigma} = \frac{S}{\sigma} \qquad (1)$$

where N is the wave action density, t the time, $\vec{C}$ the propagation velocity in the geographical space, θ the wave direction, σ the relative frequency, and C_θ and C_σ the propagation velocity in the θ- and σ-space, respectively. Therefore, on the left-hand side of equation (1), the first term represents the rate of change of wave action in time, the second term describes the spatial propagation of wave action, and the third and fourth terms stand for the refraction and changes in the relative frequencies respectively induced by depth and currents. Finally, on the right-hand side, S is the source term representing the generation and dissipation of energy density by the different processes involved.
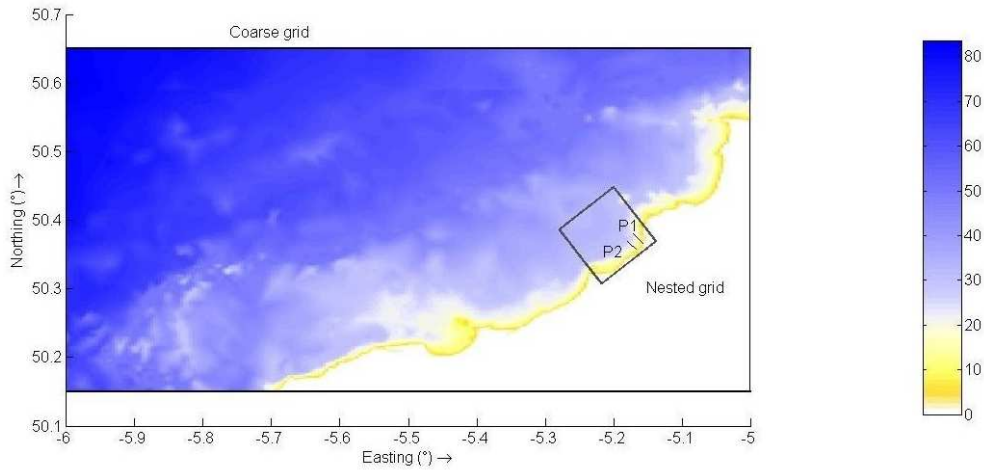
Figure 3 Computational grids of the wave propagation model [water depths in m]. Profiles P1 and P2 are shown.

In the present study two computational grids were used: (i) a coarse grid from offshore to the coast encompassing an area of approx. 100 km × 50 km with a resolution of 400 m × 200 m; and (ii) a fine, nested grid focussed on Perranporth Beach, covering an area of approx. 15 km × 15 km with a resolution of 20 m × 20 m. The high resolution of the nested grid allowed to define the position of the WECs in the array and simulate their individual wakes with accuracy. This is a prerequisite to a detailed assessment of the wave farm effects on the beach profile (Carballo and Iglesias, 2013). The bathymetric data, from the UK data centre Digimap, were interpolated onto this grid.
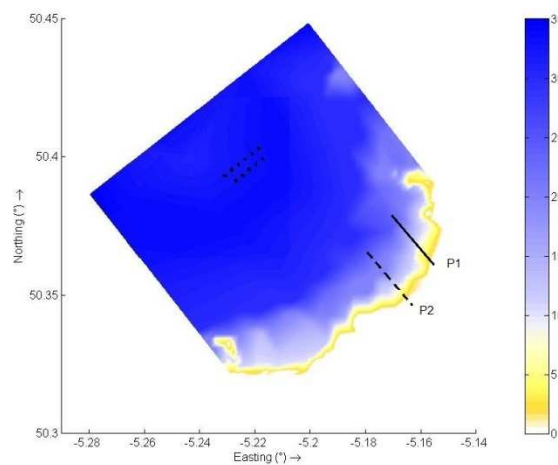

Figure 4 Schematic of wave farm considered off Perranporth Beach, at a distance of approx. 7 km from the shoreline [water depths in m]. Profiles P1 and P2 are shown.

8

To study the effects of wave energy exploitation on the beach profile an array of 11 WaveCat WECs arranged in two rows was considered. With the same layout as in Carballo and Iglesias (2013), the array was located in a water depth of 35-40 m (Figure 4). The distance between devices was 2.2D, where D = 90 m is the distance between the twin bows of a single WaveCat WEC. Finally, the wave transmission coefficient of the WECs, obtained from the laboratory tests carried out by Fernandez et al. (2012), was input into the coastal propagation model. Based on the results of these tests, which showed a very small variability in the wave transmission coefficient (with the exception of an outlier), the value K_t = 0.76 was adopted. This constitutes an approximation in that the tests carried out by Fernandez et al. (2012) did not cover all the wave conditions simulated in the present work; in future work, as more experimental data on WEC behaviour become available, this approximation will be refined.

2.3 MORPHODYNAMIC MODEL

The input conditions to XBeach were obtained from the output of the SWAN wave propagation model. XBeach is a two-dimensional model for wave propagation, long waves and mean flow, sediment transport and morphological changes of the nearshore area, beaches, dunes and back barrier during storms. XBeach concurrently solves the time-dependent short wave action balance, the roller energy equations, the nonlinear shallow water equations of mass and momentum, sediment transport formulations and bed update on the scale of wave groups (Roelvink et al., 2006).

The sediment transport is modelled with a depth-averaged advection diffusion equation (Galappatti and Vreugdenhil, 1985). The equation is:

$$\frac{\partial(hC)}{\partial t} + \frac{\partial(hCu^E)}{\partial x} + \frac{\partial}{\partial x}\left(D_s h \frac{\partial C}{\partial x}\right) + \frac{\partial(hCv^E)}{\partial y} + \frac{\partial}{\partial y}\left(D_s h \frac{\partial C}{\partial y}\right) = \frac{hC_{eq} - hC}{T_S} \qquad (2)$$

where C represents the depth-averaged sediment concentration, which varies on the wave-group time scale, D_s is the sediment diffusion coefficient, the terms u^E and v^E represent the Eulerian flow velocities, T_s is the sediment concentration adaptation time scale that depends on the local water depth and the sediment fall velocity, and C_{eq} is the equilibrium concentration, thus representing the source term in the sediment transport equation. The sediment transport formula defined by Van Thiel de Vries (2009) was used to determine the sediment equilibrium concentration.

In the present study, the model was applied in 1DH mode (x, z) to simulate the beach profile evolution. From the results of the nearshore wave propagation model, spectra with a frequency of 6 hours were obtained with and without the wave farm to compare the impact on the coast. These spectra were the input of the morphodynamic model, which provided beach profile results every 6 minutes to compare the evolution of the profile in both cases.

A varying grid size was employed in the morphodynamic model: the resolution was defined as a function of the water depth and the offshore wave conditions, and subjected to the grid size smoothness constraints. On these grounds, the Courant condition was applied to find the optimal grid size. The optimised grid was coarser in high water depths and finer in the intertidal zone, where a size of 1 m was adopted so as to accurately characterise the evolution of the profile.

Finally, to describe properly the behaviour of the beach, the time series of wave data was broken down into a number of segments. These segments were grouped into two types, Type A (Accretion) and Type E (Erosion), depending on the values of the wave parameters and the consequent nature of the beach profile changes, either accretionary or erosionary. Type A, associated with calm conditions, was set with a

10

stationary constant wave energy distribution, based on given values of root mean square wave height (H_{rms}), mean absolute wave period (T_{m01}), mean wave direction (θ_m) and directional spreading coefficient (s), obtained from the nearshore wave propagation model. Type E, associated with storm periods, used the parametric spectra as input to create time-varying wave amplitudes, i.e., the envelopes of wave groups (Van Dongeren et al., 2003). The difference in approach between the two categories is the way that wave groups were treated. Type A segments included wave groups, as they are important to describe the behaviour of the beach during erosion conditions. In contrast, wave groups were not taken into account in Type E segments because this would result in an overestimation of erosion (Baldock et al., 2010).

2.4 ASSESSMENT OF THE IMPACT OF THE WAVE FARM ON THE BEACH PROFILE

To quantify the impact of the wave farm on the beach profile the following parameters were defined: the Bed Level Impact (*BLI*), the eroded area in the baseline scenario (*A*), the eroded area in the presence of the farm (*A_f*), and the Erosion Impact (*EI*) index.

The bed level impact *(BLI,* in m*)* was defined as

$$BLI(x) = \zeta_f(x) - \zeta(x), \qquad (3)$$

where x is the horizontal coordinate along the profile, $\zeta_f(x)$ is the bed level in the presence of the farm, and $\zeta(x)$ is the bed level in the baseline scenario. The *BLI* index represents the change in the bed level drop due to the shelter afforded by the wave farm.

For their part, the eroded area in the baseline scenario (*A,* in m^3 per linear metre of beach) and the eroded area in presence of the farm *(A_f,* in m^3 per linear metre of beach*)* were defined as

$$A = \int_{x_0}^{x_{\max}} \left[\zeta_0(x) - \zeta(x) \right] dx, \qquad (4)$$

$$A_f = \int_{x_0}^{x_{\max}} \left[\zeta_0(x) - \zeta_f(x) \right] dx, \qquad (5)$$

where $\zeta_0(x)$ is the initial bed level and x_{max} and x_0 are the limits of integration, with x_{max} the maximum value of the x coordinate (which corresponds to the landward end of the profile) and x_0 the value corresponding to a bed level of 0, i.e., $\zeta(x_0) = 0$.

Finally, the Erosion Impact (*EI, in %*) index was defined as

$$EI = \frac{1}{\left(x_{\max} - x_0 \right)} \int_{x_0}^{x_{\max}} \left[\zeta_f(x) - \zeta(x) \right] \left[\zeta_0(x) - \zeta(x) \right]^{-1} dx \quad (6)$$

EI index is a dimensionless parameter that represents the reduction of the eroded area brought about by the wave farm as a fraction of the total eroded area.

3. RESULTS AND DISCUSSION

3.1 WAVE PROPAGATION MODEL

The results obtained from the nearshore wave propagation model were validated with the wave buoy data during the period from November to December 2007 and February to April 2008 owing to the lack of data during January. A very good fit was achieved between the simulated and measured time series (Figures 5 and 6). This is further confirmed by the error statistics: *RMSE = 0.46 m* and $R^2 = 0.84$ (with *RMSE* the Root Mean Square Error and R^2 the coefficient of determination).
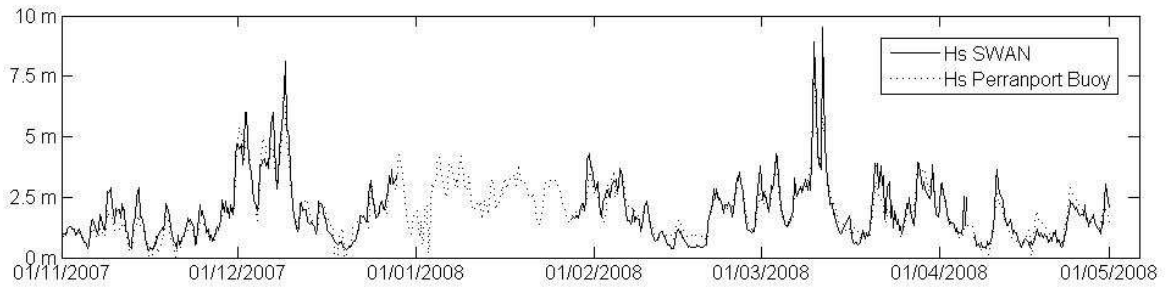
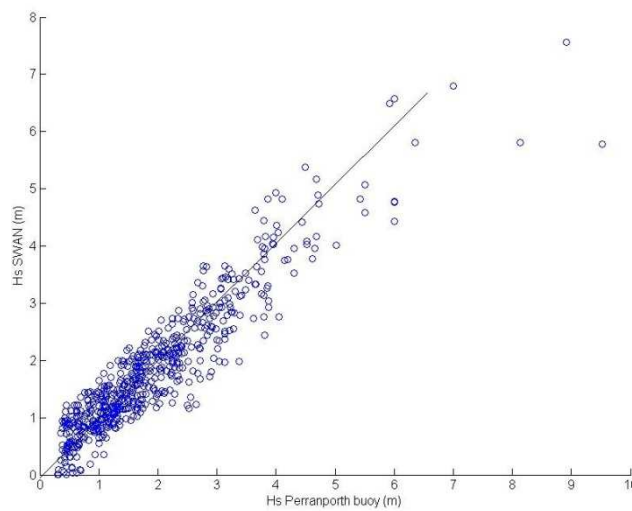**Figure 5 Time series of simulated (*Hs,SWAN*) and measured (*Hs,buoy*) significant wave height.**

Figure 6 Scatter diagram: simulated (*Hs,SWAN*) vs. measured (*Hs,buoy*) significant wave height.

Having validated the numerical model, it was used to compare the wave patterns with and without the wave farm and to determine the wave conditions that were used as input to the morphodynamic model. As an example of the effects of the wave farm on the wave patterns, the wave propagation corresponding to the peak of a storm on 10 March 2008 is shown in Figure 7. The deep water wave conditions were: significant wave height, $H_{s0} = 10.01$ m; peak wave period, $T_p = 15.12$ s; and peak wave direction, $\theta_p = 296.38$ °. A substantial decrease of the significant wave height, exceeding 30% along the wakes of the WECs, is apparent in the more detailed graph of wave farm area (Figure 8). This decrease is less marked on the beach itself. In the northern section of

13

the beach the reduction of wave height is more pronounced than elsewhere owing to the deep water wave direction (approx. WNW).
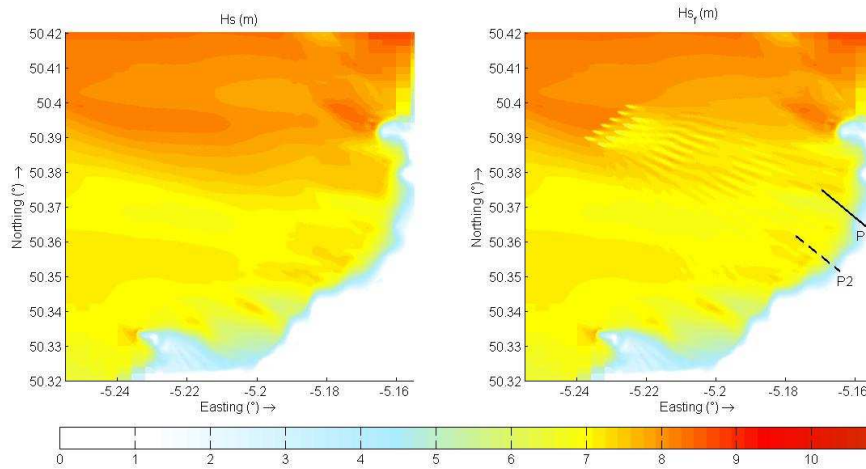

Figure 7 Significant wave height in the baseline scenario (*Hs*) and in the presence of the farm (*Hsf*) at the peak of a storm (10 Mar 2008, 18:00 UTC) [deep water wave conditions: H_{s0} = 10.01 m, T_p = 15.12 s, θ_p = 296.38 °]. Profiles P1 and P2 are shown.
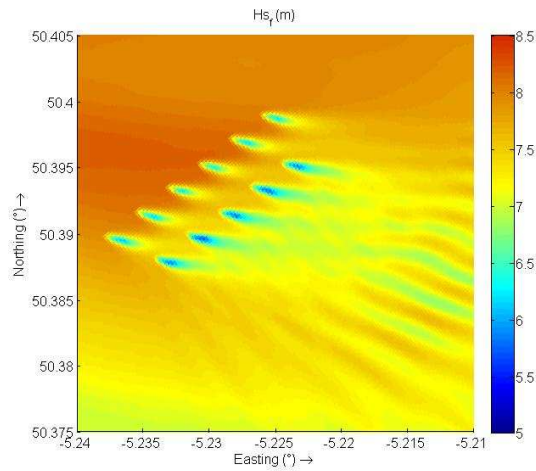

Figure 8 Significant wave height (*Hsf*) within the wave farm at the peak of a storm (10 Mar 2008, 18:00 UTC) [deep water wave conditions: H_{s0} = 10.01 m, T_p = 15.12 s, θ_p = 296.38 °].

The average reduction of the wave energy flux, *J*, during the period studied at different points along the 10 m contour is shown in Table 1. The areas most sheltered by the wave farm are the middle and, especially, northern sections of the beach. On these grounds two profiles in the northern and middle sections of Perranporth Beach were selected for the analysis of the impacts of the wave farm (Figure 2).

14

Beach Point	Coordinates		ΔH_s (%)	ΔJ (%)
	Easting (°)	Northing (°)		
North	-5.17	50.36	3.26	13.25
Middle	-5.18	50.35	1.75	7.90
South	-5.21	50.34	0.70	0.93

Table 1 Significant wave height reduction (ΔHs) and wave power reduction (ΔJ) caused by the wave farm at different points along the 10 m contour.

3.2 MORPHODYNAMIC MODEL

The impact of the wave power reduction on the beach was studied through the evolution of the two profiles of Perranporth Beach. This was carried out using the spectra generated by the wave propagation model with and without the wave farm in the morphodynamic model. The series were split, as explained in Section 2.3, to describe suitably the behaviour of the beach in different periods. The results showed that type E segments are mainly responsible for the erosion of the profiles.
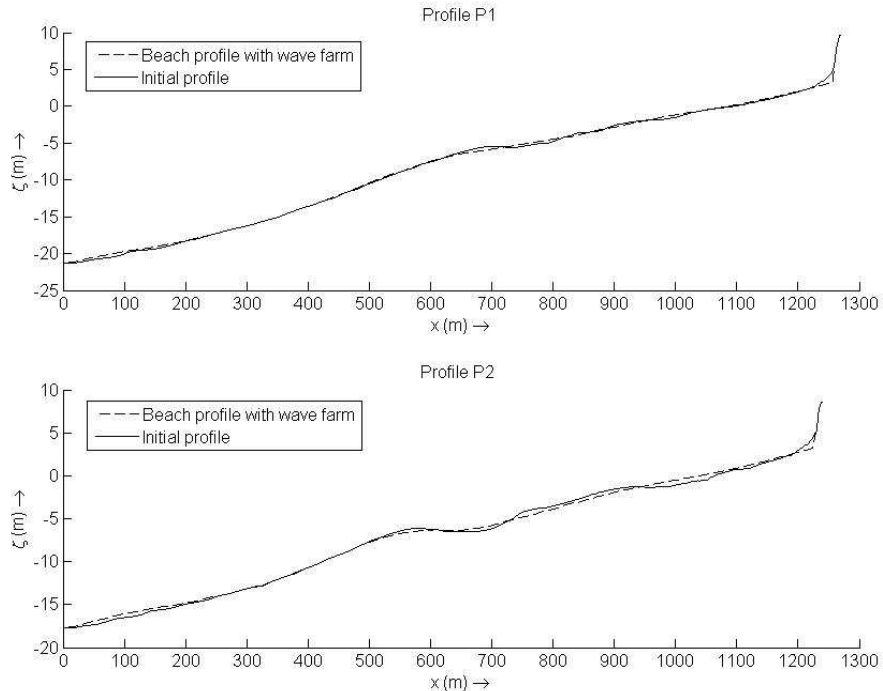

Figure 2 Bed level at Profile P1 and P2: initial [1 Nov 2007, 0000 UTC] and after three months with and the wave farm [22 Jan 2008, 15:47 UTC].

15

Figure 9 shows the evolution of the initial profiles 1 (P1) and 2 (P2) after a storm. The graph compares the initial beach profiles with those after three months of operation of the wave farm. Both graphs illustrate that the erosion of the profiles is concentrated mainly in the beach face, which is the section of the profile exposed to wave uprush. The eroded material is moved to a lower section of the profile.

To better visualise the effect of wave energy extraction, the situation of profile P2 with and without the farm is shown in Figure 10. The reduction of the wave energy flux at the beach leads to a substantial reduction (of the order of 3 m) in the erosion of the dune delineating the landward limit of the beach.
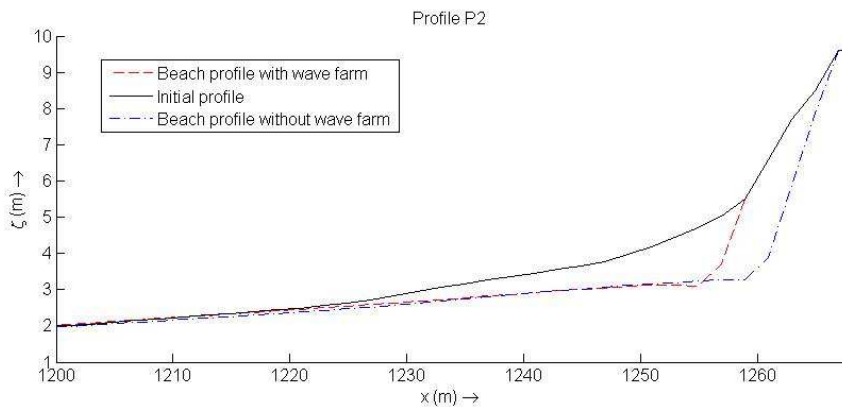

Figure 3 Beach face level at Profile P2: initial [1 Nov 2007, 0000 UTC] and after three months with and without the wave farm [22 Jan 2008, 15:47 UTC].

The impact of the wave farm on the beach profile was analysed through the parameters defined in Section 2.4. The *BLI* parameter along Profiles P1 and P2 is illustrated in Figure 11 for three different points in time: 1 month (*M1*), 3 months (*M3*) and 6 months (*M6*) after the beginning of the study period. The results for both profiles show a significant reduction of the erosion in the beach face and in the bar (around x = 600 m). The bar forms part of the response mechanism of the natural system to protect the beach face from increased wave attack. Figure 11 proves that the effect of the wave farm is a reinforcement of the bar, and therefore enhanced protection for the beach face

16

in storms. Advancing in time, the *BLI* values increase in the bar area, i.e., the aforementioned effect is intensified.
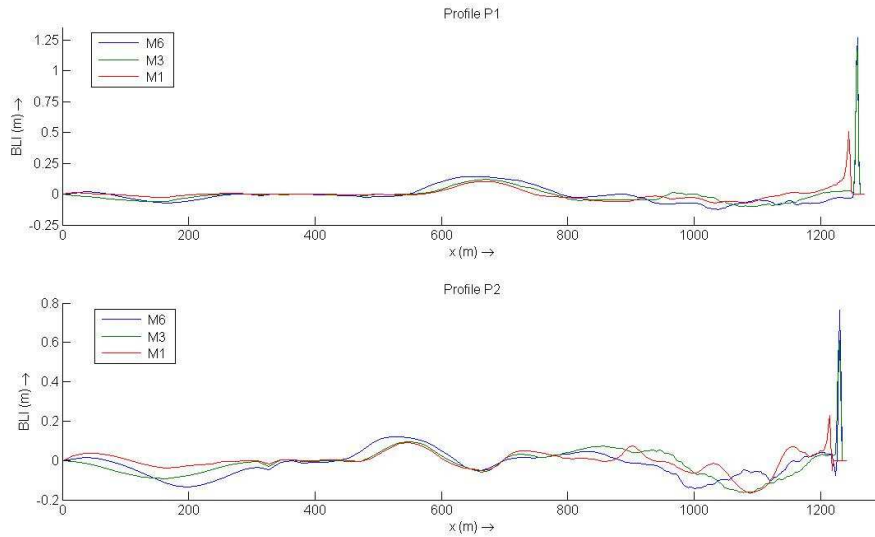

Figure 4 Evolution of *BLI* along Profiles P1 and P2 at different points in time: 1 month (*M1*), 3 months (*M3*) and 6 months (*M6*) after the beginning of the study period.

As regards the beach face, the *BLI* values for both profiles are also significant and show that the wave farm reduces the erosion. This is nowhere more apparent than on the dune at the landward end of the profile, where *BLI* values exceed 1 m. Table 2 shows the values of the eroded areas at the beach face at the same points in time as in Figure 11. It is observed for both profiles and especially in Profile P1, that the erosion is higher at the first two points in time (*M1* and *M3*) than at the last one, which is associated with less energetic conditions (Figure 5). Further, the *EI* values confirm the significant reduction in the erosion owing to the presence of the wave farm. It is also noted that the effect of the wave farm is more significant in the north of the beach (Profile P1) than in the middle of the beach (Profile P2), as may be seen in Table 1.

Profiles	M1			M3			M6		
	A	A_f	EI	A	A_f	EI	A	A_f	EI
Profile P1	20.53	14.11	31.27	16.3	10.42	36.07	23.85	18.66	21.76
Profile P2	15.69	12.91	*17.72*	21.31	16.85	*20.93*	25.53	21.42	*16.10*

Table 2 Eroded area in the baseline scenario (*A*), in the presence of the farm (*A_f*), and Erosion Impact (*EI*) index for Profiles P1 and P2 at different points in time: 1 month (*M1*), 3 months (*M3*) and 6 months (*M6*) after the beginning of the study period

The results showed a significant reduction of the erosion along profiles P1 and P2, which may indicate some degree of coastal protection owing to the presence of the wave farm nearshore. The present work was framed as the first step in the assessment of the impact of wave farms on the beach profile – a relevant aspect for the development of wave energy, and one which was not investigated to date – and the accuracy of its results will likely be enhanced in future research.

4. CONCLUSIONS

In this paper, the impact of a wave farm consisting of 11 WaveCat WECs on the beach profile was investigated through a case study. This is the first study focussed on the effect of wave energy on the beach profile evolution. A high-resolution nearshore wave propagation model was coupled to a morphodynamic model to assess the wave farm impacts over a medium-term period.

First, to study the effect of the wave farm a high-resolution grid was employed on Perranporth beach to describe properly the interaction of the wave farm and the sea. The transmission coefficient of the WEC employed was obtained through laboratory tests.

It was found that the wave farm effect varies in the different areas of the beach, affecting, in particular, the northern section of the beach and reducing its wave energy flux up to 12%. This extraction of energy modifies the coastal processes in the nearshore.

Second, a morphodynamic model was employed to investigate the impact of the wave energy extraction. Two profiles were studied, the first in the north of the beach and the second in the middle. The impact of the wave energy exploitation on the profiles was analysed through several parameters. These allowed the assessment of the impact of the wave farm on the bed level and the eroded area compared to the baseline scenario. The bed level impact (*BLI*) parameter showed a substantial effect on the bar and on the beach face. *BLI* values exceeded 1 m at some points in time. Concerning the erosion impact (*EI*) parameter, the reduction of the eroded area reached values of up to 35% at the first points in time (*M1* and *M3*) and 21% at the last (*M6*) in the north of the beach. In the middle of the beach the reduction was lower, reaching values up to 20% at the first points in time (*M1* and *M3*) and 16% at the end of the period studied (*M6*).

This substantial reduction in the erosion of the profiles constitutes an added benefit of the wave farm. This is corroborated by the results of the present work, which dealt with the impacts of a relatively small, hypothetical wave farm (with 11 WECs distributed in an area of 1.5km^2); despite its size, the wave farm was shown to have a significant effect in reducing the erosion of the beach face. This effect would likely be even more significant in the case of a larger wave farm.

In conclusion, a wave farm can be considered a *green* alternative to conventional forms of coastal protection, in the sense that it provides not only some degree of coastal protection but also *green* (carbon-free) energy. This synergy enhances the viability of wave farms.

5. Bibliography

Austin, M. et al., 2010. Temporal observations of rip current circulation on a macro-tidal beach. Continental Shelf Research, 30(9): 1149-1165.

Baldock, T.E., Manoonvoravong, P. and Pham, K.S., 2010. Sediment transport and beach morphodynamics induced by free long waves, bound long waves and wave groups. Coastal Engineering, 57(10): 898-916.

Booij, N., Ris, R.C. and Holthuijsen, L.H., 1999. A third-generation wave model for coastal regions: 1. Model description and validation. Journal of Geophysical Research: Oceans, 104(C4): 7649-7666.

Carballo, R. and Iglesias, G., 2013. Wave farm impact based on realistic wave-wec interaction. Energy, 51: 216-229.

Clément, A. et al., 2002. Wave energy in europe: Current status and perspectives. Renewable and Sustainable Energy Reviews, 6(5): 405-431.

Cornett, A.M., 2008. A global wave energy resource assessment. ISOPE--579

Cowell, P. and Thom, B., 1994. Morphodynamics of coastal evolution. Cambridge University Press, Cambridge, United Kingdom and New York, NY, USA.

Egbert, G.D., Bennett, A.F. and Foreman, M.G., 1994. Topex/poseidon tides estimated using a global inverse model. Journal of Geophysical Research: Oceans (1978–2012), 99(C12): 24821-24852.

European Commission, 2007. A european strategic energy technology plan (set-plan)–towards a low-carbon future, Communication from the Commission to the Council, the European Parliament, the European Economic and Social Committee and the Committee of the Regions, COM (2007).

Falcão, A.F.O., 2007. Modelling and control of oscillating-body wave energy converters with hydraulic power take-off and gas accumulator. Ocean Engineering, 34(14–15): 2021-2032.

Falcão, A.F.O. and Justino, P.A.P., 1999. Owc wave energy devices with air flow control. Ocean Engineering, 26(12): 1275-1295.

Fernandez, H. et al., 2012. The new wave energy converter wavecat: Concept and laboratory tests. Marine Structures, 29(1): 58-70.

Galappatti, G. and Vreugdenhil, C., 1985. A depth-integrated model for suspended sediment transport. Journal of Hydraulic Research, 23(4): 359-377.

Gonzalez, R., Zou, Q. and Pan, S., 2012. Modelling of the impact of a wave farm on nearshore sediment transport. Proceedings of the international conference of Coastal Engineering 2012.

Iglesias, G. and Carballo, R., 2009. Wave energy potential along the death coast (spain). Energy, 34(11): 1963-1975.

Iglesias, G. and Carballo, R., 2010. Offshore and inshore wave energy assessment: Asturias (n spain). Energy, 35(5): 1964-1972.

Iglesias, G. and Carballo, R., 2011. Choosing the site for the first wave farm in a region: A case study in the galician southwest (spain). Energy, 36(9): 5525-5531.

Iglesias, G., Carballo, R., Castro, A. and Fraga, B., 2008. Development and design of the wavecat™ energy converter. Coastal Engineering: 3970-3982.

Jamal, M.H., Simmonds, D.J., Magar, V. and Pan, S., 2011. Modelling infiltration on gravel beaches with an xbeach variant. Proceedings of the International Conference on Coastal Engineering, 1(32): sediment. 41.

Kofoed, J.P., Frigaard, P., Friis-Madsen, E. and Sørensen, H.C., 2006. Prototype testing of the wave energy converter wave dragon. Renewable Energy, 31(2): 181-189.

McCall, R.T. et al., 2010. Two-dimensional time dependent hurricane overwash and erosion modeling at santa rosa island. Coastal Engineering, 57(7): 668-683.

Mendoza, E. et al., 2014. Beach response to wave energy converter farms acting as coastal defence. Coastal Engineering, 87(0): 97-111.

Millar, D.L., Smith, H.C.M. and Reeve, D.E., 2007. Modelling analysis of the sensitivity of shoreline change to a wave farm. Ocean Engineering, 34(5-6): 884-901.

Nørgaard, J.H., Andersen, T.L. and Kofoed, J.P., 2011. Wave dragon wave energy converters used as coastal protection, Proceedings of the international conference of Coastal Structures 2011. Imperial College Press., Yokohama.

Pender, D. and Karunarathna, H., 2012. Modeling beach profile evolution – a statistical–process based approach. 2012.

Pender, D. and Karunarathna, H., 2013. A statistical-process based approach for modelling beach profile variability. Coastal Engineering, 81(0): 19-29.

Pontes, M. et al., 1996. Weratlas–atlas of wave energy resource in europe. Report to the European Commission, JOULE II Programme, 96p.

Reeve, D.E. et al., 2011. An investigation of the impacts of climate change on wave energy generation: The wave hub, cornwall, uk. Renewable Energy, 36(9): 2404-2413.

Roelvink, D. et al., 2009. Modelling storm impacts on beaches, dunes and barrier islands. Coastal Engineering, 56(11–12): 1133-1152.

Roelvink, J. et al., 2006. Xbeach model description and manual. UNESCO-IHE Institute for Water Education.

Ruol, P., Zanuttigh, B., Martinelli, L., Kofoed, P. and Frigaard, P., 2011. Near-shore floating wave energy converters: Applications for coastal protection, Proceedings of the international conference of Coastal Engineering 2010, Shanghai.

Scott, T., Masselink, G. and Russell, P., 2011. Morphodynamic characteristics and classification of beaches in england and wales. Marine Geology, 286(1–4): 1-20.

Thorpe, T., 2001. The wave energy programme in the uk and the european wave energy network.

Tolman, H.L., 2002. User manual and system documentation of wavewatch-iii version 2.22.

Van Dongeren, A.R., Battjes, J. and Svendsen, I., 2003. Numerical modeling of infragravity wave response during delilah. Journal of Geophysical Research, 108(C9): 3288.

Van Thiel de Vries, J., 2009. Dune erosion during storm surges. PhD Thesis Thesis, Delft University of Technology.

Vicinanza, D., Contestabile, P. and Ferrante, V., 2013. Wave energy potential in the north-west of sardinia (italy). Renewable Energy, 50: 506-521.

Vidal, C., Méndez Fernando, J., Díaz, G. and Legaz, R., 2007. Impact of santoña wec installation on the littoral processes. Proceedings of the 7th European wave and tidal energy conference, Porto, Portugal.

Williams, J.J., de Alegría-Arzaburu, A.R., McCall, R.T. and Van Dongeren, A., 2012. Modelling gravel barrier profile response to combined waves and tides using xbeach: Laboratory and field results. Coastal Engineering, 63(0): 62-80.

Zanuttigh, B. and Angelelli, E., 2013. Experimental investigation of floating wave energy converters for coastal protection purpose. Coastal Engineering, 80: 148-159.